Science World Journal Vol. 17(No 1) 2022
www.scienceworldjournal.org
ISSN: 1597-6343 (Online), ISSN: 2756-391X (Print)
Published by Faculty of Science, Kaduna State University

IMPROVEMENT OF PORCELAIN PHYSICAL PROPERTIES THROUGH THE SUBSTITUTION OF QUARTZ ELEMENT WITH RICE HUSK ASH AND PALM OIL FUEL ASH

* H.U. Jamo, I.D. Umar, Abdu S., Zainab Ali Tambalo, Sani Abdulkarim, Ibrahim T. Salisu, Aminu Musa Liman, M.B. Abdullahi, Izzudden M.

Department of Physics, Kano University of Science and Technology Wudil, PMB 3244, Kano, Nigeria

*Corresponding Author Email Address: jamouhfce@gmail.com

ABSTRACT
Rice husk ash (RHA) and palm oil fuel ash (POFA) have a great potential to replace the quartz element in porcelain composition. The Malaysian RHA and POFA were used to substitute quartz in porcelain body from 0 wt% to 25 wt%. The mixed powder was pressed into pellets at pressure of 91 MPa. All the pellets were sintered at a temperatures of 1000 ºC, 1100 ºC, 1200 ºC and 1300 ºC for soaking time 2 hours. The physical analysis results show that the physical properties of the samples increased with increase in substitution and also with the increase in temperature. Moreover, maximum physical properties were obtained on 20 wt% substitution of quartz by RHA and POFA at a temperature of 1200 ºC. The XRD results show that RHA was mainly amorphous form as indicated by a broad peak, while the pattern for POFA indicated the crystalline phase. The SEM shows both RHA and POFA particles consist of irregular particles and have porous cellular It could be concluded therefore, that the RHA and POFA have significant role in the enhancing the physical properties of porcelain body.

Keywords; Feldspar, Kaolin, POFA, Quartz, RHA

INTRODUCTION

Porcelain ceramics is a highly vitrified ceramic material produced from a body formulated by mixtures of kaolin, quartz and feldspar. The kaolin [$Al_2Si_2O_5$ $(OH)_4$], gives plasticity to the ceramic mixture; flint or quartz (SiO_2), maintains the shape of the formed article during sintering; and feldspar [$(K,Na)_2O$. Al_2O_3. $6H_2O$], serves as flux (as and Dana, 2003). These three constituents place porcelain in the phase system [$(K, Na)_2O$-Al_2O_3-SiO_2)] in terms of oxide constituents, hence the term triaxial porcelain ceramic (Buchanan, 1991). The main phase composition of a porcelain body is constituted by a heterogeneous glassy matrix and needle shaped mullite crystals together with some quartz grains and closed irregular shaped pores. Mullite crystals, which are derived from the solid-state decomposition of the clay reacting with feldspar, are endowed with excellent mechanical, creep, thermal and chemical properties. Because of the complex interplay between raw materials, processing routes and the kinetics of the firing process, porcelains represent some of the most complicated ceramic systems (Jamo *et al.,* 2015; Edwards *et al.,* 2022).

The quest over the period of time has been to increase mechanical strength, and to reduce the production costs. In most efforts to increase strength, emphasis has been placed on minimization of quartz in the porcelain formula because of the β to α phase inversion of quartz which occurs at 573 ºC during cooling. The inversion results into decrease of quartz particle volume and may lead to cracks in the body (Olorunyolemi *et al.,* 2022). So far, there are reports of improvements in the mechanical properties by reducing the use of quartz. These include replacements of quartz with kyanite (Schroeder, 1978), Al_2O_3 (Kobayashi *et al.,* 1994 and Das and Dana. 2003: Navak *et al.,* 2022), RHA (Prasad *et al.,* 2001, Jamo *et al.,* 2014; Jamo *et al.,* 2015; Noh *et al.,* 2016), sillimanite sand (Maity and Sarkar, 1996), fly ash (Dana *et al.,* 2004), partial replacement of feldspar and quartz by fly ash and blast furnace slag (Dana *et al.,* 2005), silica fume (Prasad *et al.,* 2002: Olorunyolemi *et al.,* 2022), with a mixture of rice husk ash (RHA) and silica fume (Prasad *et al.,* 2003). Furthermore, it is understood that an attempt was made to part of quartz with fired porcelain by Stathis *et al*., (2004) which yield a non-positive result on the bending strength.

However, due to the rich silica content of RHA and POFA, this study wishes to investigate the influence of the combination of these ashes on physical properties of porcelain at different temperature.

MATERIALS AND METHODS

Experimental

The rice husk (RH) was thoroughly washed with distilled water in order to remove adhering soil and dust. After that it was dried in an oven at 100°C for 24 hours. Then the dried husk was subjected to the chemical treatment; 2M HCL, 5% solid at 25 °C before calcinations to increase silica content. After the leaching process, the treated husk was washed with distil water and then dried again. The treated husk was then subjected to calcinations at 700°C for six (6) hours.

The POFA was dried in an oven at 100 ºC for 24 hours. After that it was be grounded in a ball mill to reduce the needed particle size to improve reactivity. The milling time was approximately 90 minutes at 200 rpm. Afterwards, the materials were subjected to a set of sieves less than 50 µm in order to remove the particles coarser than 50 µm. The untreated POFA was heated at a temperature of 600 ºC for 1.5 hours in an electric furnace to remove excess carbon.

Porcelain powder was grounded separately in a ball mill. The powder was sieved using sieve shaker and dried in an oven. The RHA and POFA was gradually incorporated into the body of porcelain powder from 0 %wt, to 25 %wt (Table 1). The composition was mixed using a ball mill for one and half hours. The mixed powder was pressed into pellets at mould pressure of 91 MPa. All the pellets were sintered at a temperature of 1000 ºC, 1100 ºC, 1200 ºC and 1300 ºC for the soaking times of 2 h at a heating rate of 5 ºC per minute. The compressive strength was determined.

The chemical composition of the raw materials was studied using X-Ray Fluorescence (XRF) machine. The machine (XRF Bruker

S4 Pioneer) was operated at 60 KV. The powders of samples were pressed into pellets with ratio 8:2, powder to wax. The mould pressure used in producing the pellets is 8 tonnes and hold time is one minute. The samples were placed in the XRF machine for elemental analysis.

The XRD instrument in this work is Bruker D8 Advance X-diffractometer. It is operated at 40 kV. The ground powder was mounted on a glass slide located at the centre of the diffraction chamber. The sample was exposed to Cu Kα radiation (λ=1.5404 Å) in reflection mode and reflections are recorded by detector. When the sample rotates in the same direction at half angular velocity 2θ o min-1 , the sample rotates in the same direction at half angular velocity of the detector, θ o , in order to keep the detector at the focusing point of the diffracted X-rays. The chart recorder records the intensities and 2θ o values of the diffracted peaks simultaneously with the rotation.

Table 1: The composition with the substitution of quartz by RHA and POFA (wt %)

Sample name	Kaolin	Feldspar	Quartz	RHA	POFA
AP1	50	25	25	0	0
AP2	50	25	20	3	2
AP3	50	25	15	6	4
AP4	50	25	10	9	6
AP5	50	25	5	12	8
AP6	50	25	0	15	10

RESULTS AND DISCUSSION

The presence of various elements within the raw materials can be seen from the table. This table shows the result of XRF analysis of kaolin, feldspar, quartz, RHA and POFA. It is evident that SiO_2 is the major composition in all the raw materials: kaolin, feldspar, quartz, RHA and POFA with 69.3 wt%, 72.7 wt%, 99.4 wt%, 93.7 wt% and 66.9 wt% and then followed by alumina with 24.3 wt%, 16.4 wt%, 0.2 wt%, 2.1 wt% and 6.4 wt% respectively.

Table 2: XRF Analysis

Sample	Content											
Oxides	SiO_2	Al_2O_3	K_2O	P_2O_5	CaO	MgO	CO_2	SO_3	FeO_3	Na_2O	TiO_2	LOI
RHA	93.70	2.11	1.18	0.96	0.81	0.53	010	0.45	-	-	-	0.16
POFA	66.91	6.44	5.20	3.72	5.56	3.13	-	0.33	5.72	0.19	-	2.30
Kaolin	69.30	24.30	2.44	-	-	-	0.10	-	0.27	-	0.27	0.36
Feldspar	72.70	16.40	0.50	2.42	-	-	-	6.87	0.40	0.29	-	0.10
Quartz	99.40	0.22	-	-	-	-	0.10	-	-	-	-	0.28

Figure 1 (a,b,c and d) shows the XRD pattern of POFA, RHA, porcelain raw material and control sample respectively. The XRD pattern of POFA (Fig.1) shows crystalline phases as indicated by the presence of the elemental peaks of quartz (ICDD 046-1045), calcite (ICDD 005-0586) and portlandite ICDD 044-1481). A similar pattern was reported by Das and Dana, (2004). As it can be seen from Figure(b) represent the XRD pattern of RHA reveals an amorphous structure as indicated by a broad peak. This is in line with the result obtained by Foo and Hameed (2009).

The phase concentration is indicated by the peak height, which represents higher concentration. Pattern (c) represents the XRD of the porcelain raw material the major phases identified are quartz (ICDD 046-1045), mullite (ICDD 074-4143) and kaolinite (ICDD 006-0221) similar report was obtained by Jamo *et. al.* (2013). The control sample is represented by XRD pattern (d) where the phases present are quartz (ICDD 046-1045), mullite (ICDD 074-4143) and cristobalite (ICDD 082-0512) .

Science World Journal Vol. 17(No 1) 2022
www.scienceworldjournal.org
ISSN: 1597-6343 (Online), ISSN: 2756-391X (Print)
Published by Faculty of Science, Kaduna State University

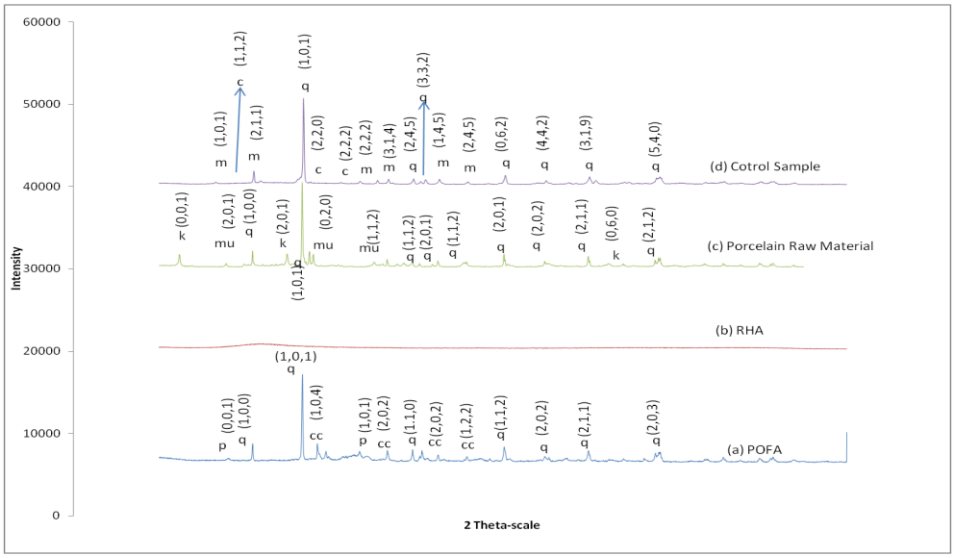

Figure 1: The XRD of POFA, RHA, Porcelain Raw Materials and Control Sample materials (where c = cristobalite, cc = calcite, k = kaolin, m = mullite, mu = muscovite, p = portlandite, q = quartz)

PARTICLE SIZE ANALYSIS

Porcelain raw material

Figure 2 shows the median particle size (d_{10}) and (d_{60}) of RHA are 1.06 µm and 8.12 µm respectively. The average particle size (d_{30}) is 2.99 µm.

RHA

Figure 3 shows the median particle size (d_{10}) and (d_{60}) of RHA are 2.18 µm and 11.33 µm respectively. The average particle size (d_{30}) is 5.35 µm.

POFA

Figure 4 shows the median particle size (d_{10}) and (d_{60}) of RHA are 1.31 µm and 15.36 µm respectively. The average particle size (d_{30}) is 5.40 µm.

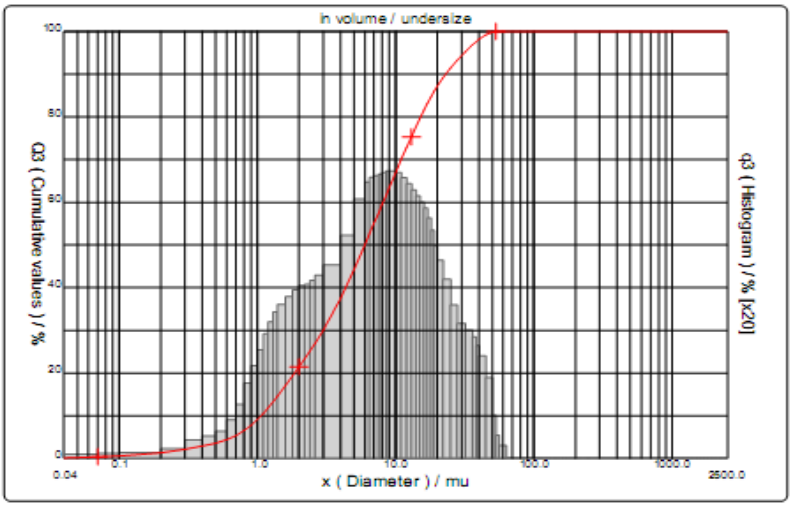

Figure 2. Result of particle size analysis of porcelain raw material

Science World Journal Vol. 17(No 1) 2022
www.scienceworldjournal.org
ISSN: 1597-6343 (Online), ISSN: 2756-391X (Print)
Published by Faculty of Science, Kaduna State University

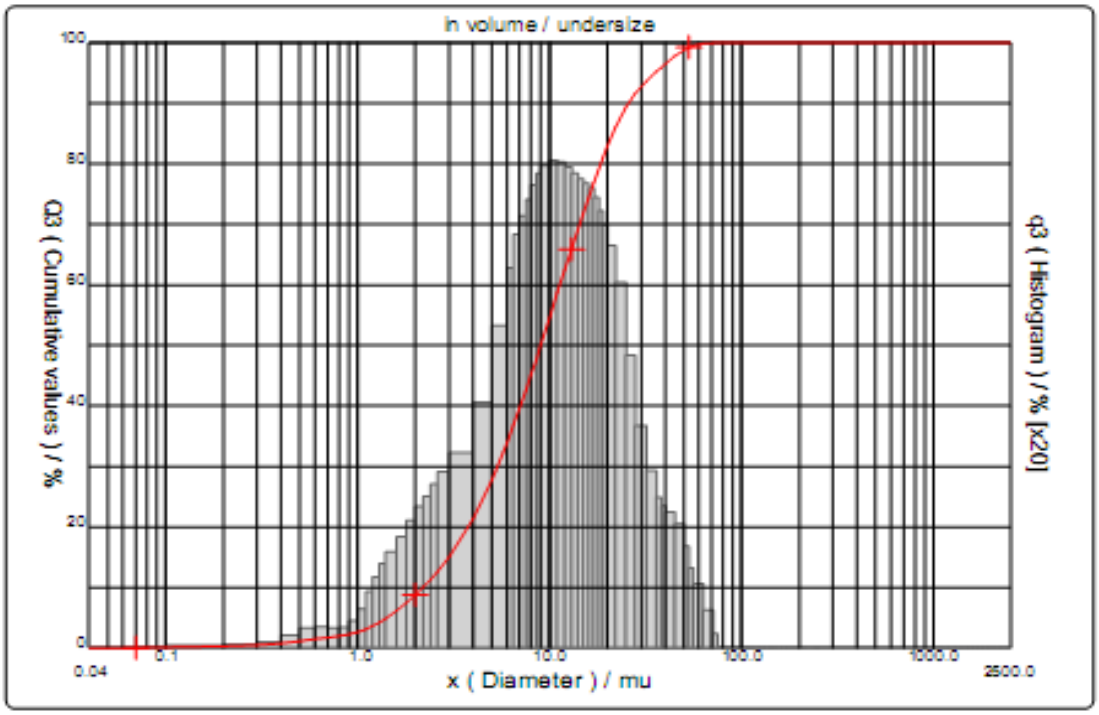

Figure 3: Result of particle size analysis of RHA

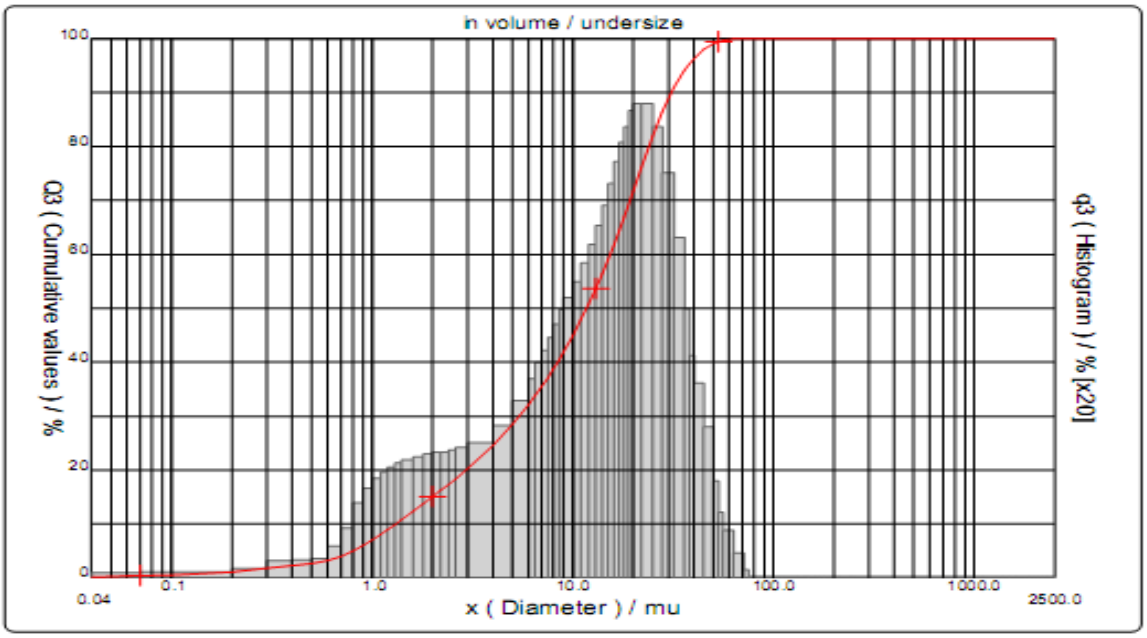

Figure 4: Result of particle size analysis of POF

Science World Journal Vol. 17(No 1) 2022
www.scienceworldjournal.org
ISSN: 1597-6343 (Online), ISSN: 2756-391X (Print)
Published by Faculty of Science, Kaduna State University

Scanning electron microscopy (SEM)

Figure 5 (a) Shows the SEM image of RHA material. The image reveals irregular particles with porous cellular. Figure 5 (b) shows the SEM image of the treated POFA particles; the particles were irregular in shape and having porous texture. In addition, no agglomeration of POFA particles after the heat treatment as can be seen in the Figure. Figure 5 (c) shows the SEM image Porcelain raw materials consist of crushed irregular particles.

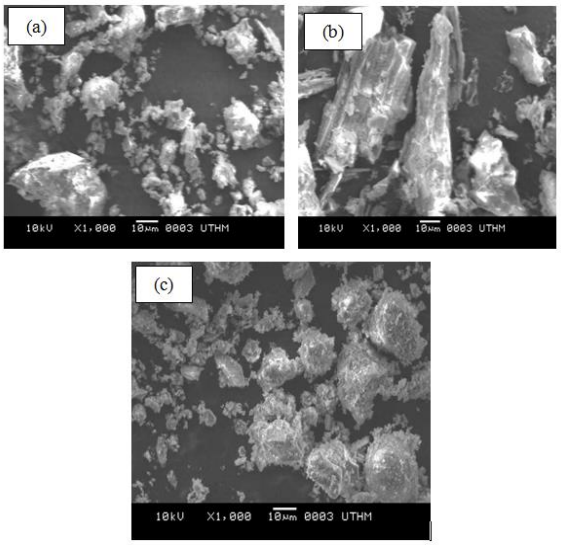

Figure 5: Surface morphology SEM of (a) RHA (b) POFA (c) ceramic (porcelain) raw material. Phase 1: Substitution of quartz by RHA

As shown in Figure 6, the porosity decreases with substitution of quartz with RHA and POFA. The experiment was carried out according to ASTM C373. The porosity decreased with increase in replacement of quartz with RHA and POFA. The minimum porosity was achieved with approximate values of 3.9%, 3.0%, 2.8% and 3.4% at the temperature of 1000 ^{o}C, 1100 ^{o}C, 1200 ^{o}C and 1300 ^{o}C respectively, on 20 wt% of RHA and POFA. At 25 wt% of RHA the porosity increases because of glassy phase formation. Similarly, the porosity decreases as the temperature increases from 1000 ^{o}C to 1200 ^{o}C. But as the temperature increases to 1300 ^{o}C the porosity increases due to bloating.

In fact, open porosity decreases with increasing temperature and the substitution due to the formation of a glassy phase that is mainly originated from the feldspar and the ashes (RHA and POFA). Noh *et al.,* (2016) reported that the increasing temperature causes both an increase in liquid phase amount and a decrease in liquid phase viscosity. Under the surface energy forces created by the fine pores contained in the ceramic body, the liquid phase tends to approach the particles and, therefore, open porosity decreases. Close porosity increases as the temperature reaches 1300 ^{o}C because of the body bloating due to the pressure of the gas inside the closed pores, which tends to expand the pores. This type of relationship had been shown by previous studies (Noh *et al.,* 2017; Jamo *et al.,* 2015: de Azevedo *et al.,* 2022).

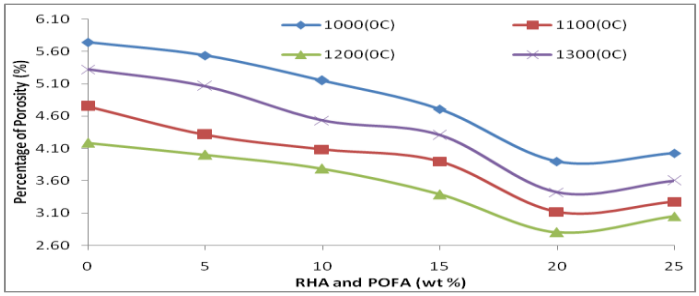

Figure 6: Effect of temperature on percentage of porosity of the samples with different percentage of RHA and POFA

Figure 7 shows the result of bulk density versus RHA and POFA content of the sintered samples. In line with the porosity result presented in Figure 2, The bulk density increases from 2.28 g/cm^3 to 2.38 g/cm^3 at a temperature of 1000 ^{o}C on 20 wt% of RHA and POFA. This as a result of metakaolin transformation to a spinal-type structure. At the temperature of 1100 ^{o}C the maximum bulk density values was achieved with 2.42 g/cm^3. Similarly, at the temperature of 1200 ^{o}C with an approximate value of 2.43 ^{o}C the maximum bulk density was recorded on 20 wt% of RHA and POFA. This reduces the maturing temperature to 1200 ^{o}C compared to 1300 ^{o}C found in the literature. Sintering is a process of consolidation of particles under the temperatures below the melting point and is caused mostly by solid-state reactions. During sintering solid bonds are formed between particles. Such bonding reduces the surface energy by reducing the free surface. In this process, the grain boundaries are partially eliminated through grain growth and the pore volume is reduced, leading to a condensed mass. The bulk density increases as the replacement increases between 0 wt% and 20 wt%, substitution above 20 wt% causes the bulk density to decrease. Replacement above 20 wt% causes the values of bulk density to drop due to excess glassy formation.

The bulk density increases with increase in temperature, as the temperature increases from 1000 ^{o}C to 1200 ^{o}C and decreases after reaching maximum at a temperature of 1300 ^{o}C. The required temperature to induce such bonding depends upon the characteristics of both starting materials and the particle size distribution (Kamseu *et al.,* 2007; Noh *et al.* 2017: Li *et al.,* 2022). Solid-state sintering takes place between particles of single or multiple phases, where homogenization takes place during the sintering of mixed phases that form a single-phase product.

However, authors such as Martín-Márquez *et al.* (2010); and Romero *et al.* (2006), asserted that in many cases, sintering takes place in the presence of a liquid phase, especially when many phases are present, and is known as liquid-phase sintering. The behaviour of this result is similar to the bulk density result presented in Figure 4. The bulk density increases with substitution and temperature reaches maximum and decreases. The progressive substitution of RHA and POFA, and the increase in temperature,

contributes to the increase of bulk density. This could be attributed to the increasing formation of glassy phase to the detriment of the crystalline ones. The liquid phase aids in sintering, thereby increasing consolidation at high temperatures (Jamo *et al.*,2015; Noh *et al.,* 2016; Noh *et al.,* 2017: Nayak *et al.,* 2022).

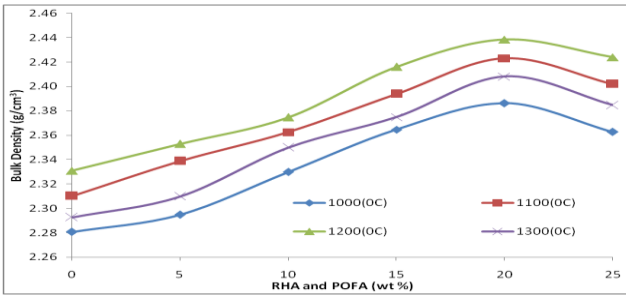

Figure 7: Effect of temperature on bulk density of the samples with different percentage of RHA and POFA

CONCLUSION

The effective substitution of quartz by RHA and POFA in porcelain body have greatly increased the physical properties of the material body. In addition, these properties increasing temperature. The maximum physical properties for porcelain samples containing RHA and POFA occurred at a temperature of 1100 ^{O}C, on 20 wt% substitution. The typical sequece enhanced densification with increasing temperature contributed to the increase in physical properties. Densification of the porcelain body takes place at the temperature of 1100 ºC. The increase in the physical properties and the substantial decrease in porosity of the mixes containing RHA and POFA, are attributed to the glassy formation and densification of the individual grains during the vitrification process.

ACKNOWLEDGEMENT

The authors would like to acknowledge the financial support of Universiti Tun Hussein Onn Malaysia. We would also like to thank the following Mr. Mohd Azrul Nizam bin Mustari, Mr. Fazlannuddin Hanur bin Harith, Mr. Shahrul Mahadi bin Samsudin, Mr. Mohd Tarmizi bin Nasir, Mr. Anuar bin Ismail, Mr. Ahmad Nasrull bin Mohamed, Norsidah Binti Harun, and Nooriskandar for their assistance as laboratory staff.

REFERENCES

Buchanan, W. T., Svare, C. W., & Turner, K. A. (1981). The effect of repeated firings and strength on marginal distortion in two ceramometal systems. *Journal of Prosthetic Dentistry*, *45*(5), 502-506.

Dana, K., & Das, S. K. (2004). Evolution of microstructure in flyash-containing porcelain body on heating at different temperatures. *Bulletin of Materials Science*, *27*(2), 183-188.

Dana, K., Dey, J., & Das, S. K. (2005). Synergistic effect of fly ash and blast furnace slag on the mechanical strength of traditional porcelain tiles. *Ceramics International*, *31*(1), 147-152.

Das, S. K., & Dana, K. (2003). Differences in densification behaviour of K-and Na-feldspar-containing porcelain bodies. *Thermochimica Acta*, *406*(1-2), 199-206.

de Azevedo, A. R., Amin, M., Hadzima-Nyarko, M., Agwa, I. S., Zeyad, A. M., Tayeh, B. A., & Adesina, A. (2022). Possibilities for the application of agro-industrial wastes in cementitious materials: a brief review of the Brazilian perspective. *Cleaner Materials*, *3*, 100040.

Edwards, H. G. (2022). *Porcelain Analysis and Its Role in the Forensic Attribution of Ceramic Specimens*. Cham, Switzerland: Springer.

Jamo, H. U., Noh, M. Z., & Ahmad, Z. A. (2014). Influence of Temperature on the Substitution of Quartz by Rice Husk Ash (RHA) in Porcelain Composition. In *Applied Mechanics and Materials* (Vol. 465, pp. 1297-1303). Trans Tech Publications.

Jamo, H. U., Noh, M. Z., & Ahmad, Z. A. (2015, April). Effect of Mould Pressure and Substitution of Quartz by Rice Husk Ash on the Bulk Density and Compressive Strength of Porcelain Body. In *Materials Science Forum* (Vol. 819).

Kamseu, E., Leonelli, C., Boccaccini, D. N., Veronesi, P., Miselli, P., Pellacani, G., & Melo, U. C. (2007). Characterisation of porcelain compositions using two china clays from Cameroon. *Ceramics international*, *33*(5), 851-857.

Kobayashi, Y., Ohira, O., Satoh, T., & Kato, E. (1994). Effect of quartz on the sintering and bending strength of the porcelain bodies in quartz-feldspar-kaolin system. *Journal of the Ceramic Society of Japan*, *102*(1181), 99-104.

Li, X. (2022). Influence of inner crown thickness on the bonding strength of porcelain fused to Co-Cr alloy endocrown. *Journal of Oral Science*, *64*(1), 40-43.

Martín-Márquez, J., Rincón, J. M., & Romero, M. (2010). Mullite development on firing in porcelain stoneware bodies. *Journal of the European Ceramic Society*, *30*(7), 1599-1607.

Nayak, S. K., Satapathy, A., & Mantry, S. (2022). Use of waste marble and granite dust in structural applications: A review. *Journal of Building Engineering*, *46*, 103742.

Noh, M. Z., Jamo, H. U., & Ahmad, Z. A. (2016). The Hardness Properties of Porcelain with Substitution of Quartz by Rice Husk Ash at Different Soaking Time. In *Materials Science Forum* (Vol. 840, pp. 39-43). Trans Tech Publications.

Noh, M. Z., Jamo, H. U., & Ahmad, Z. A. (2016). The Hardness Properties of Porcelain with Substitution of Quartz by Rice Husk Ash at Different Soaking Time. In *Materials Science Forum* (Vol. 840, pp. 39-43). Trans Tech Publications.

Noh, M. Z., Jamo, H. U., & Ahmad, Z. A. (2017). The Bending Strength of the Porcelain with the Substitution of

Quartz by Palm Oil Fuel Ash. In *Materials Science Forum* (Vol. 888, pp. 112-116). Trans Tech Publications.

Noh, M. Z., Jamo, H. U., & Ahmad, Z. A. (2017). The Bending Strength of the Porcelain with the Substitution of Quartz by Palm Oil Fuel Ash. In *Materials Science Forum* (Vol. 888, pp. 112-116). Trans Tech Publications.

Olorunyolemi, O. C., Ogunsanya, O. A., Akinwande, A. A., Balogun, O. A., & Kumar, M. S. (2022). Influence of SiO2 form the rice husk ash and coal fly ash particles on the mechanical behaviour and grain characteristics of the stir-casted hybrid composites.

P Horch, A., & Terossi, M. (2022). Population structure, maturity and relative growth of the porcelain crab Pachycheles laevidactylus Ortmann, 1892 (Decapoda, Porcellanidae) in a temperate zone. *Marine Ecology*, e12693.

Prasad, C. S., Maiti, K. N., & Venugopal, R. (2001). Effect of rice husk ash in whiteware compositions. *Ceramics International*, *27*(6), 629-635.

Romero, M., Martín-Márquez, J., & Rincón, J. M. (2006). Kinetic of mullite formation from a porcelain stoneware body for tiles production. *Journal of the European Ceramic Society*, *26*(9), 1647-1652.

Schroeder, J. E. (1978). Inexpensive high-strength electrical porcelain. *AMERICAN CERAMIC SOCIETY BULLETIN*, *57*(5), 526-526.

Stathis, G., Ekonomakou, A., Stournaras, C. J., & Ftikos, C. (2004). Effect of firing conditions, filler grain size and quartz content on bending strength and physical properties of sanitaryware porcelain. *Journal of the European Ceramic Society*, *24*(8), 2357-2366.

Usman Jamo, H. (2015). *Mechanical properties of ceramics tiles by replacement of quartz by RHA and POFA* (Doctoral dissertation, Universiti Tun Hussein Onn Malaysia).